Journal of Geophysical Research: Biogeosciences

RESEARCH ARTICLE
10.1029/2018JG004438

Warming-Induced Earlier Greenup Leads to Reduced Stream Discharge in a Temperate Mixed Forest Catchment

Ji Hyun Kim[1,2,3], **Taehee Hwang**[1], **Yun Yang**[4], **Crystal L. Schaaf**[5], **Emery Boose**[6], **and J. William Munger**[7]

[1]Department of Geography, Indiana University, Bloomington, IN, USA, [2]Department of Earth and Environment, Boston University, Boston, MA, USA, [3]Department of Civil and Environmental Engineering, Yonsei University, Seoul, South Korea, [4]USDA-Agricultural Research Service, Beltsville, MD, USA, [5]School for the Environment, College of Science and Mathematics, University of Massachusetts Boston, Boston, MA, USA, [6]Harvard Forest, Harvard University, Petersham, MA, USA, [7]School of Engineering and Applied Sciences and Department of Earth and Planetary Sciences, Harvard University, Cambridge, MA, USA

Abstract The phenological response of vegetation to ongoing climate change may have great implications for hydrological regimes in the eastern United States. However, there have been few studies that analyze its resultant effect on catchment discharge dynamics, separating from dominant climatic controls. In this study, we examined the net effect of phenological variations on the long-term and interannual gross primary production (GPP) and evapotranspiration (ET) fluxes in a temperate deciduous forest, as well as on the catchment discharge behavior in a mixed deciduous-conifer forest catchment. First, we calibrated the spring and autumn leaf phenology models for the Harvard Forest in the northeastern United States, where the onsets of greenup and senescence have been significantly advanced and delayed, 10.3 and 6.0 days respectively, over the past two decades (1992–2011). We then integrated the phenology models into a mechanistic watershed ecohydrological model (RHESSys), which improved the interannual and long-term simulations of both the plot-scale daily GPP and ET fluxes and the catchment discharge dynamics. We found that the phenological changes amplified the long-term increases in GPP and ET driven by the climatic controls. In particular, the earlier greenup onsets resulted in increases in annual ET significantly, while the delayed senescence onsets had less influence. Consequently, the earlier greenup onsets reduced stream discharge not only during the growing season but also during the following dormant season due to soil water depletion. This study highlights the importance of understanding vegetation response to ongoing climate change in order to predict the future hydrological nonstationarity in this region.

Key Points:
- Both carbon and water fluxes were better simulated when phenological variations were incorporated into a watershed hydrology model
- The long-term increase of GPP and ET fluxes due to climate drivers were amplified by the extended growing season
- Earlier greenup onset reduced catchment discharge not only during growing season but also during the following dormant season

Supporting Information:
- Supporting Information S1

Correspondence to:
J. H. Kim,
kim.jk237@gmail.com

Citation:
Kim, J. H., Hwang, T., Yang, Y., Schaaf, C. L., Boose, E., & Munger, J. W. (2018). Warming-induced earlier greenup leads to reduced stream discharge in a temperate mixed forest catchment. *Journal of Geophysical Research: Biogeosciences*, *123*, 1960–1975. https://doi.org/10.1029/2018JG004438

Received 6 FEB 2018
Accepted 24 MAY 2018
Accepted article online 30 MAY 2018
Published online 29 JUN 2018

1. Introduction

Vegetation phenology is a distinct ecosystem response to a changing climate (Menzel et al., 2006), and a major driver for the exchange of carbon, water, and energy between terrestrial ecosystems and the atmosphere (Penuelas et al., 2009; Richardson et al., 2010). Many studies have documented that warming temperatures have lengthened growing seasons (GSs) over the past three decades (Buitenwerf et al., 2015; Walther et al., 2002), including a 7–13 days longer GS across the eastern United States (Elmore et al., 2016; Richardson et al., 2006). The implications of longer GS on key terrestrial ecosystem processes have also been investigated, indicating an enhanced annual carbon uptake in temperate deciduous forests of about 7.3 g C/m^2 per additional GS day (Baldocchi, 2008; Churkina et al., 2005; Keenan et al., 2014; Polgar & Primack, 2011; Richardson et al., 2009; White et al., 1999). Although evidence of increased carbon uptake has been consistent, the effect of an extended GS on hydrologic cycles appears to be more complicated (Hogg et al., 2000; Keeling et al., 1996). Transpiration through the open vegetation stomates would increase during lengthened periods of full canopy (Berry et al., 2010; Wilson & Baldocchi, 2000), and evaporation from the vegetated surfaces (i.e., interception) would increase as well. Soil evaporation from the ground floor would be expected to decrease as a result of decreased solar radiation penetrating through closed canopies and lower ground temperatures due to longer canopy duration (Huntington, 2010; Penuelas et al., 2009). Changes in these energy and surface water fluxes should also be associated with adjustments in soil water storage, which then could have a cascading effect on the magnitude of groundwater recharge and stream discharge (*Q*; Creed et al., 2014; Richardson et al., 2012; Thompson et al., 2011).

There have been, however, few studies that attempt to separate the climatic and phenological controls on plot-scale evapotranspiration (ET) and on watershed discharge in the eastern United States where seasonal cycles in vegetation water use exceed annual variation in precipitation. Several studies have shown that the annual ET of deciduous forests is positively correlated with the phenological variation (Migliavacca et al., 2012; Richardson et al., 2013; White et al., 1999), while others have suggested little influence (Puma et al., 2013). Likewise, watershed-scale ET estimates based on mass balance appear to reflect increasing or decreasing trends across the eastern United States (Huntington & Billmire, 2014; Jones et al., 2012; Kramer et al., 2015; Lu et al., 2015). However, watershed-scale ET estimates include, by their nature, transient storage changes, which are greatly affected by the interannual hydroclimate variability (e.g., precipitation intensity and timing; Hwang et al., 2018; Troch et al., 2009). Therefore, watershed-scale ET estimates may not be the most proper measure to quantitatively assess the net effect of interannual phenological changes on key hydrological fluxes under ongoing climate changes.

There have been even fewer studies that have addressed the effect of phenological changes on subsequent seasonal stream discharge dynamics. Czikowsky and Fitzjarrald (2004) showed that the streamflow recession time (the time to return to the base flow levels after rainfall) has shortened and the diurnal streamflow amplitude has increased in the northeastern United States, resulting from earlier vegetation greenup onsets and the increased water use. Creed et al. (2015) reported that streamflow during the spring and autumn has declined in a temperate forest in Canada, and the timing of Budyko dryness index (the ratio of potential evaporation to precipitation, PET/P) and evaporative index (P-Q/P) had shifted to earlier in the spring and later in the autumn. However, such empirical approaches are limited in their ability to quantify the net changes in stream discharge driven by phenological variations due to hydroclimate variability. To date, few studies have incorporated dynamic vegetation phenology models into watershed models as a main driver of streamflow dynamics, even though several studies have discussed this apparent link (Huntington et al., 2004; Thompson et al., 2011). Moreover, most studies have not considered the cooccurring effect of enhanced vegetation growth, due to lengthened GS s, on the hydrological fluxes. It is only very recent that a distributed modeling framework was applied to separate the effect of vegetation dynamic and hydroclimate variability, showing that lengthened GS and subsequent vegetation growth can account for long-term nonstationary hydrologic behavior in forested watersheds in southeastern United States (Hwang et al., 2018). Therefore, it is critical to improve our understanding of the implication of phenological changes on hydrological behavior across different climate regions through the use of a unified framework that includes both vegetation dynamics and watershed-scale hydrological processes (Migliavacca et al., 2012; Richardson et al., 2012, 2013).

In this study, we integrated a phenology model into a mechanistic watershed-scale ecohydrological model. We then evaluated the model results at a mixed forest catchment using both plot- and catchment-scale field measurement data. Finally, we assessed the net phenological controls on the long-term and interannual hydrological fluxes (i.e., ET and stream discharge) within the unified modeling framework.

2. Data and Method

2.1. Study Site

The study site is the Arthurs Brook (previously known as Bigelow Brook) catchment located within the Harvard Forest Long Term Ecological Research (LTER) site in New England (Figure 1). The climate is generally cool and moist with the annual mean temperature of 8.5°C (ranging from −7 to 20°C) and an annual total precipitation of about 1,100 mm evenly distributed throughout the year (the period of record of 1964–2016; Boose, 2018a; Boose & Gould, 2004). Over the past two decades, both the GS daytime temperature and the annual total precipitation have increased by 0.1 and 5.5% per decade, respectively (Keenan et al., 2013). The study catchment has a moderate topography (elevation ranging from 240 to 430 m above sea level). It is mostly covered by a 3 m depth of glacial till over gneiss and schist bedrock, which texture is a largely sandy loam (National Resources Conservation Service, 2009). The study catchment has an area of 65.9 ha with 51.5% of deciduous broadleaf forest (dominated by northern red oak [*Quercus rubra*] and red maple [*Acer rubrum*]), 44% of evergreen needleleaf forest (dominated by eastern hemlock [*Tsuga canadensis*] and white pine [*Pinus strobus*]), and 4.5% of woody wetlands (a mix of hardwoods and shrub). These tree stands range from 70 to 220 years in age and are on average 25 m tall (Hadley et al., 2008; Urbanski et al., 2007). The invasive insect, the Hemlock

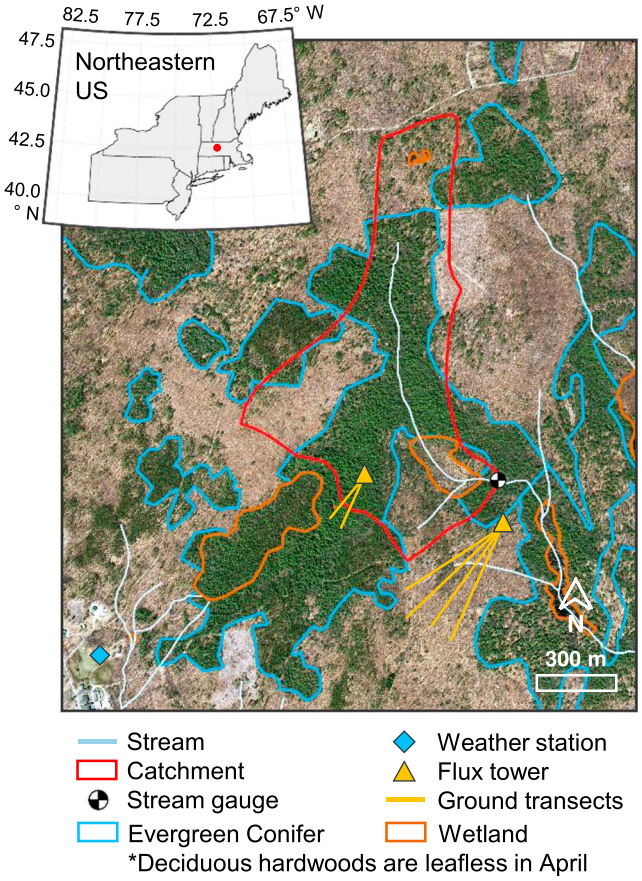

Figure 1. A study catchment (red boundary) at the Harvard Forest in the northeastern United States. The aerial photo was taken in April 2009 before the greenup (available at http://maps.massgis.state.ma.us) and clearly shows the distribution of evergreen forest and woody wetlands (brown boundary; available at http://harvardforest.fas.harvard.edu). Flux and ground data were measured at two eddy-covariance flux tower (the Environmental Measurement Site, EMS, tower at 42.5378°N, 72.1715°W in the right yellow triangle; the Hemlock tower (HEM) at 42.5393°N, 72.1779°W in the left yellow triangle) and along ground transects leading to each flux tower (yellow lines). Data are listed in Table S1.

woolly adelgid (*Adelges tsugae*), was first observed at this study site in 2002. The ET of the hemlock-dominated area began to decrease significantly in 2012, whereas the annual stream discharge started to increase in 2013 due to the infestation (Kim et al., 2017). Therefore, in this study, we focused on the period from 1992 to 2011 prior to the significant impact on ET fluxes by the ongoing Hemlock woolly adelgid infestation.

2.2. Field Data

We used daily climate data (max and min temperatures and total precipitation; available from the LTER data archive; Boose, 2018a; Boose & Gould, 2004) for both the phenology and ecohydrological models. Additional meteorological data, such as atmospheric CO_2 concentrations, vapor pressure deficit, wind speed, and photosynthetically active radiation, has been collected at two eddy-covariance flux towers at Harvard Forest (Figure 1): the Environmental Measurement Site (EMS) tower since 1991 (Munger & Wofsy, 2017) and the Hemlock (HEM) tower since 2004 (Munger & Hadley, 2017). For the calibration and validation of the ecohydrological model, we used the daily stream discharge data determined from water level measurements (Boose, 2018b). Water levels have been measured every 10 s since December 2007, and 15-min averaged water levels are then converted to stream discharge using standard flow rating curves.

We compared the simulated gross primary productivity (GPP) and ET with the data from the two towers (EMS and HEM). Details of the data processing of the flux data (i.e., quality control, flux corrections, and gap-filling) are described elsewhere (Barford, 2001; Urbanski et al., 2007). For the EMS tower data, we used the gap-filled hourly GPP estimates, and we filled short-term ($\leq$2 hr) gaps in the ET measurements via linear interpolation, while leaving longer ($>$2 hr) gaps unfilled. For the HEM tower data, we used the half-hourly GPP and ET data from only the evergreen forest-dominated upwind area (the compass directions of 180 to 270°), and short-term gaps were filled via linear interpolation. The two tower data have been shown to represent the carbon and water fluxes of each plant biome type: a deciduous broadleaf forest by the EMS tower and an evergreen coniferous forest by the HEM tower (Keenan et al., 2013). From the hourly (or half-hourly) data, we calculated the daily GPP (g C/m^2) and ET (mm) for the days without any gap and removed GPP and ET on rainy days (and the days immediately after the rainy days) to prevent rainfall-associated biases (Loescher et al., 2005). We also used ground measurements (leaf area index [LAI], soil respiration, and soil temperature) that have been collected in transects within the area where each plant biome type dominates (Figure 1). The list of all data sets used in this study is in Table S1, and all data sets are available through the Harvard Forest Data Archive (http://harvardforest.fas.harvard.edu/harvard-forest-data-archive).

2.3. Leaf Observations and the Phenology Models

We estimated spring and autumn phenology indices (PIs) using data from 20 years of visual leaf observations (O'Keefe, 2015). Details of the leaf observations are described elsewhere (Keenan et al., 2014; Richardson et al., 2009). We used the data only of the two dominant deciduous hardwood species (red oak and red maple) located within 2 km of the EMS tower (three stands for each species; $n = 6$). The spring PI was defined from 0 (no budburst) to 1 (leaves fully expanded) based on the percentage of leaf size relative to fully grown leaves. The autumn PI varies from 1 (no color change) to 0 (complete coloration) based on the percentage of leaves that have changed color. The daily PI was calculated by taking the median of the PIs of all monitored trees on the same observation date.

Using these *PIs*, we examined four types of sigmoidal logistical functions with different input variables to determine the onsets of leaf greenup and senescence (Richardson et al., 2006). Daily mean temperature data were used to calculate degree-day temperature sums (DD), including heating degree-day (HDD; degree-day sums above 4°C since 1 January) and chilling degree-day (CDD; degree-day sums below 4°C since 15 August), for each spring and autumn. The first phenological model only considered the day of year (DOY; i.e., x_1 = DOY in equation (1)), and the second model also had one variable (x_1 = HDD or CDD for the spring or autumn, respectively). The third model was based on both the DOY and one DD (x_1 = DOY and x_2 = HDD or CDD for the spring or autumn, respectively), and the fourth model took all the variables into account for both the spring and autumn (x_1 = DOY, x_2 = HDD, and x_3 = CDD),

$$\mathrm{PI} = \frac{1}{1 + \exp\left(c_0 - \sum_{i=1}^{n} c_i x_i\right)} \tag{1}$$

where x_i is the independent variable (DOY, HDD, and CDD), n is the number of independent variables (i.e., 1 in both first and second models and 2 and 3 in the third and fourth models, respectively), c_i is the coefficient for the variable, and c_0 is the scale coefficient. We used these PIs for the first 10 years (1992–2001) to estimate the coefficients in the four different models and then used the following 10 years (2002–2011) of the indices to validate the calibrated models. The coefficients were calibrated using iterative least squares estimation (*nlinfit* function in Matlab; The MathWorks, 2000). The best model was selected for greenup and senescence, respectively, based on the coefficient of determination (R^2) and the root-mean-squared-error (RMSE).

We used the curvature change of the phenology model to determine the timing of greenup and senescence onsets, with the DOYs determined by the inflection points of the spring and autumn logistic models, respectively (Figure S1; Hwang, Song, Bolstad, et al., 2011; Hwang, Song, Vose, et al., 2011; Zhang et al., 2003). The significance of the long-term trends in the greenup and senescence onsets was determined by Spearman's Rho and Mann-Kendall tests. The onset DOYs of the greenup and senescence in 1992 (the beginning of the study period) were calculated from the long-term trends, as the initial phenological states.

2.4. Distributed Ecohydrological Model

The Regional Hydro-Ecologic Simulation System (RHESSys) is a process-based distributed ecohydrological model that simulates carbon, water, and nitrogen cycles at a watershed-scale (Tague & Band, 2004). RHESSys integrates a number of biotic and abiotic processes from several submodels: MT-Clim to extrapolate plot-scale climate measurements to the landscape based on elevation, aspect, and slope (Running et al., 1987), Biome-BGC to account for plot-scale carbon and water cycles (Running & Hunt Jr., 1993; White et al., 2000), $\mathrm{CENTURY}_{\mathrm{NGAS}}$ to simulate long-term soil carbon and nitrogen processes (Parton et al., 1993, 1996), and a Distributed Hydrology Soil Vegetation Model (DHSVM) to explicitly simulate the lateral hydrologic flows following topographic gradients over landscapes (Wigmosta et al., 1994). Besides the aboveground vertical fluxes (e.g., GPP and ET), carbon and nitrogen are also transported laterally with both surface and subsurface lateral flows between adjacent patches (the simulation units) as forms of dissolved organic and inorganic matter (Lin et al., 2015). RHESSys has been successfully applied to simulate biogeochemical fluxes in a wide range of ecosystems and climate regions (Band et al., 2001; Christensen et al., 2008; Hwang et al., 2008; Hwang et al., 2009; Tague & Grant, 2009; Tague et al., 2004; Vicente-Serrano et al., 2015; Zierl et al., 2007).

The stream networks and catchment boundaries were delineated from a 30-m digital elevation model that was created by resampling a 1-m light detection and ranging (LiDAR) bare-earth surface model (http://www.mass.gov; Figure 1). We classified the forested landscapes into deciduous and evergreen forests using an aerial photo taken at the end of a dormant season (April 2009; Figure 1). The wetland boundary was provided by the Harvard Forest LTER (Foster & Boose, 1999). Model parameters for soil physical characteristics and vegetation physiological characteristics were taken from the literature and from on-site field measurements (Tables S2 and S3; Dingman, 2009; National Resources Conservation Service, 2009). Initial soil carbon and nitrogen stores were determined by spinning up the model for 500 years until it reached an equilibrium state. Initial vegetation carbon and nitrogen stores were calibrated using a 30-m LAI measurements in August 2000 (Cohen et al., 2006) and allometric equations (Munger & Wofsy, 2018).

We integrated the spring and autumn phenology models into the deciduous forest patches in RHESSys framework (30-m gridded patches). The model simulates the daily LAI value based on the fixed photosynthate from the previous day and subsequent processes (e.g., allocation, water, or nutrient limitation; Tague & Band, 2004). The key hydrological model parameters (e.g., a saturated hydraulic conductivity at the surface and its decay rate with soil depth at both vertical and lateral dimensions) were calibrated using the generalized likelihood uncertainty estimation (GLUE) method (Beven & Binley, 1992). Random parameter sets of 3,000 were generated from uniform distributions of prescribed parameter ranges. Then, acceptable (often referred as "behavioral") parameter sets were selected based on the Nash-Sutcliffe efficiency (Nash & Sutcliffe, 1970) for log-transformed daily stream discharge (NSE_{log} threshold of 0.65), which emphasizes the model performance at low flow periods when vegetation water use is tightly coupled with soil moisture dynamics (calibration period: May 2008–April 2010). The behavioral model runs were evaluated with three performance measures: NSE, NSE_{log}, and RMSE. We also validate the behavioral model runs using field measurements (stream discharge data of May 2008–April 2012, daily GPP and ET from the two towers, and ground-measured LAI and soil respiration) in the deciduous and evergreen forests, respectively, using performance measures such as r^2, RMSE, and percent bias (PBIAS $= \sum_{i=1}^{n} \left(Y_i^{obs} - Y_i^{sim}\right) * 100 \Big/ \sum_{i=1}^{n} Y_i^{obs}$, where n is the number of data) each year.

2.5. Model Implementations With "Static" and "Dynamic" Phenology Schemes

The model was implemented at a daily scale under two phenology schemes, "static" and "dynamic," with the same climate data and the hydrological/ecophysiological parameters (Tables S2 and S3). These two modeling schemes were designed to separate phenological and climatic controls on the key carbon and water fluxes within our modeling framework. Under the static phenology scheme, the model was run with the fixed greenup and senescence onsets (initial year on the long-term trend) without any interannual variation. Under the dynamic phenology scheme, the model was run with the interannually variable greenup and senescence onsets from the integrated phenology model. The model parameters were calibrated only under the static phenology scheme, assuming that hydrologic parameters do not change with different vegetation dynamics. Daily-scale model implementation allowed us to capture the resultant changes in the fluxes due to the difference in the phenology onsets by a few days.

First, we assessed the long-term increases in annual GPP and ET of the deciduous forest under the two phenology schemes (ΔGPP, ΔET in calendar year), validated using the tower-based GPP estimates. We also checked whether there was a long-term trend in the difference of the simulated catchment discharge (ΔQ) by comparing the dynamic and static phenology simulation results at a vegetation year basis. Vegetation year (from May to April of the following year in this study) has been known as an effective way to minimize the effect of soil water storage changes (Troch et al., 2009), when analyzing annual-scale water mass balance (Hwang et al., 2014, 2018; Kelly et al., 2016; Patric & Reinhart, 1971). We then examined the correlation between the phenological variations (greenup and senescence) and the net annual flux changes (ΔGPP, ΔET, and ΔQ) using an ordinary least-squared regression to examine the phenological controls on the key flux variables. We further analyzed the effect of the greenup and senescence onset variations on the hydrologic fluxes (i.e., ΔET and ΔQ) during each season: early GS (April–July), late GS (August–November), and dormant season (December–March of the following year).

3. Results

3.1. Phenology Model Performance

The first and second phenology models (one independent variable: DOY, DD) indicated excellent although somewhat poorer performances than other models (R^2 = 0.920–0.980 and 0.956–0.962 for the spring and autumn, respectively; Figure S2). The third model (two independent variables: DOY and either HDD for the spring or CDD for the autumn) provides the best fit, accounting for more than 97% of the variation in the observed phenology (R^2 = 0.982 and 0.973 for the spring and autumn, respectively). There was no apparent improvement in the model performance when using all the variables (the fourth model; R^2 = 0.981 and 0.960 in the spring and autumn, respectively).

During the study period, the simulated greenup and senescence onsets were between DOY 131 and 156 (median: 144), and between DOY 275 and 288 (median: 281), respectively (Figure 2). Significant long-term

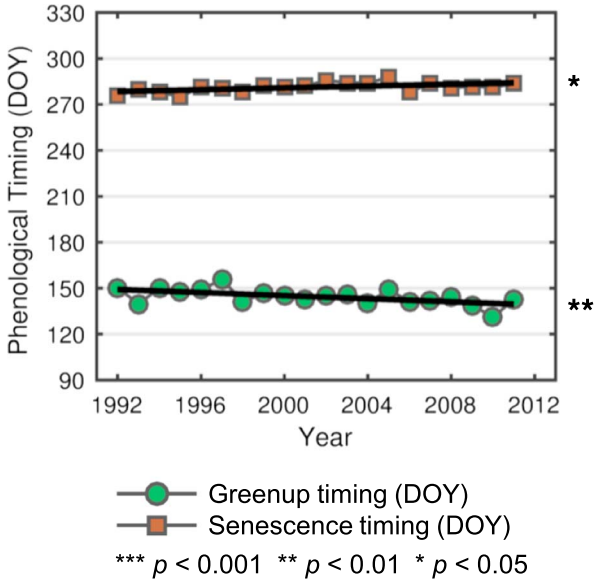

Figure 2. Phenological timing (greenup and senescence as day of year, DOY) and their long-term trends from 1992 to 2011 (black solid line). The long-term trend and its significance (asterisk) were calculated using Spearman's Rho test and Man-Kendall test.

trends were found in both timings, with a 5.1-day earlier greenup onset per decade ($p < 0.01$) and a 3.0-day delayed senescence onset per decade ($p < 0.05$). There was no significant correlation between the greenup and senescence onsets ($p > 0.05$). For the long-term trends, the greenup and senescence onsets in 1992 were DOY 149 and 278, respectively, which were the phenological dates used for the static phenology scheme.

3.2. Ecohydrological Model Performance

The simulated daily GPP for the deciduous forest (dynamic phenology) matched well with the tower-based estimates throughout the study period (r^2 = 0.88–0.95, RMSE = 1.05–1.85 g C · m^{-2} · day^{-1}, PBIAS < ±14.6%; Figure 3). The simulated daily ET of the deciduous forest (dynamic phenology) also agreed well with the tower measurements (r^2 = 0.69–0.91, RMSE = 0.35–1.15 mm/day, PBIAS < ±17.3%; Figure 4). These RHESSys model performances under the dynamic phenology scheme consistently improved as compared to model runs under the static phenology scheme (r^2 = 0.85–0.94, RMSE = 1.15–2.07 g C · m^{-2} · day^{-1}, PBIAS < ±20.9% for GPP; r^2 = 0.70–0.89, RMSE = 0.36–1.15 mm/day, PBIAS < ±19.8% for ET). In particular, the performance improvements (higher r^2 and lower RMSE) under the dynamic phenology scheme were noticeable when the greenup onsets

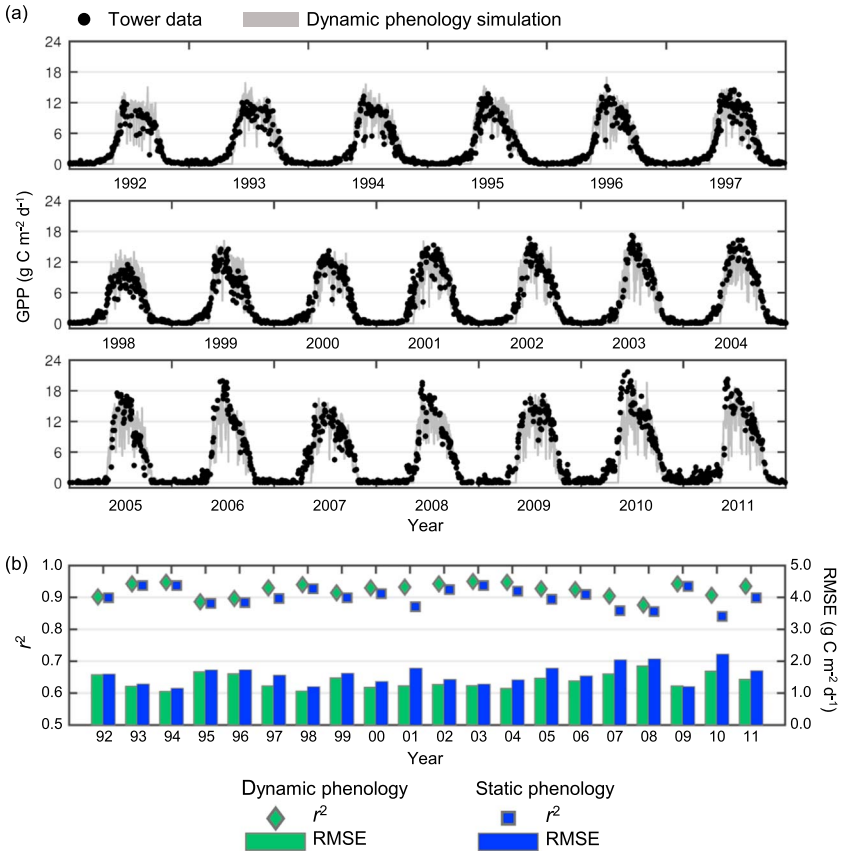

Figure 3. (a) Simulated (grey area) and measured (black dots) daily gross primary productivity (GPP) of the deciduous forest under the dynamic phenology scheme. The grey areas represent 95% confidence intervals from the behavior model runs (n = 146). (b) Statistics associated with the simulation under the dynamic (green) and static (blue) phenology schemes in each year (r^2 in symbol and RMSE in bar).

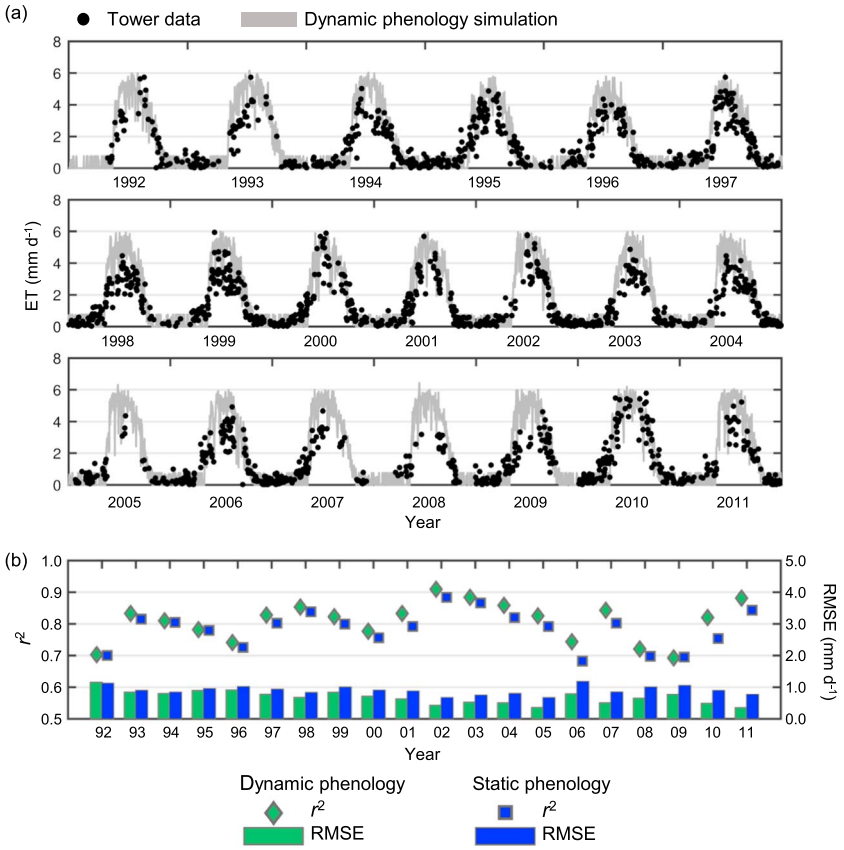

Figure 4. (a) Simulated (grey area) and measured (black dot) daily evapotranspiration (ET) of the deciduous forest under the dynamic phenology scheme. The grey areas represent 95% confidence intervals from the behavior model runs (n = 146). (b) Statistics associated with the simulation under the dynamic (green) and static (blue) phenology schemes in each year (r^2 in symbol and RMSE in bar).

began very early (e.g., 2010; Figures 3b and 4b). The model also well simulated the daily GPP and ET from the evergreen forest (r^2 = 0.87–0.98, RMSE = 0.23–0.63 g C · m^{-2} · day^{-1}, PBIAS < ±7.1% for GPP; r^2 = 0.75–0.96, RMSE = 0.29–0.79 mm/day, PBIAS < ±22.5% for ET; for a seven-year period; Figure S3). The simulated mean annual GPP was about 1487.9 ± 188.1 and 1199.7 ± 124.4 g C · m^{-2} · year^{-1} at the deciduous (dynamic phenology) and evergreen forests, respectively. The simulated mean annual ET was about 660.4 ± 50.4 and 591.0 ± 53.5 mm/year at the deciduous (dynamic phenology) and evergreen forests, respectively.

The model (dynamic phenology) also well simulated the deciduous forest LAI (r^2 = 0.78–0.97, RMSE = 0.43–1.15 m^2/m^2, PBIAS < ±20.1%; Figure S4). The measured LAI was 4.6 ± 0.41 m^2/m^2 between July and August during the study period, where about half of the interannual variations in the summer LAI was accounted for by the model (r^2 = 0.48, RMSE = 0.23 m^2/m^2). The simulated LAI under the dynamic phenology scheme agreed better with the field measurements than the simulated ones under the static phenology scheme (r^2 = 0.76–0.93, RMSE = 0.57–1.11 m^2/m^2, PBIAS < ±21.8%). The measured LAI at the evergreen forest (4.2 and 4.7 m^2/m^2 in 2008 and 2009 August, respectively) was also close to the simulated LAI (4.5–4.6 m^2/m^2; Figure S4). The simulated soil respiration has relatively good agreement with the field measurements at both the deciduous (dynamic phenology) and evergreen forests (r^2 = 0.63–0.83, RMSE = 0.71–1.40 g C · m^{-2} · day^{-1}, PBIAS < ±23.3%; Figure S5). Incorporation of the dynamic phenology slightly improved the soil respiration simulations at the deciduous forest, as compared to the static phenology scheme (r^2 = 0.59–0.80, RMSE = 0.85–1.42 g C · m^{-2} · day^{-1}, PBIAS < ±23.6%). The simulated mean annual soil respiration was about 823.2 ± 77.7 and 427.8 ± 48.35 g C/m^2 at the deciduous (dynamic phenology) and evergreen forests, respectively.

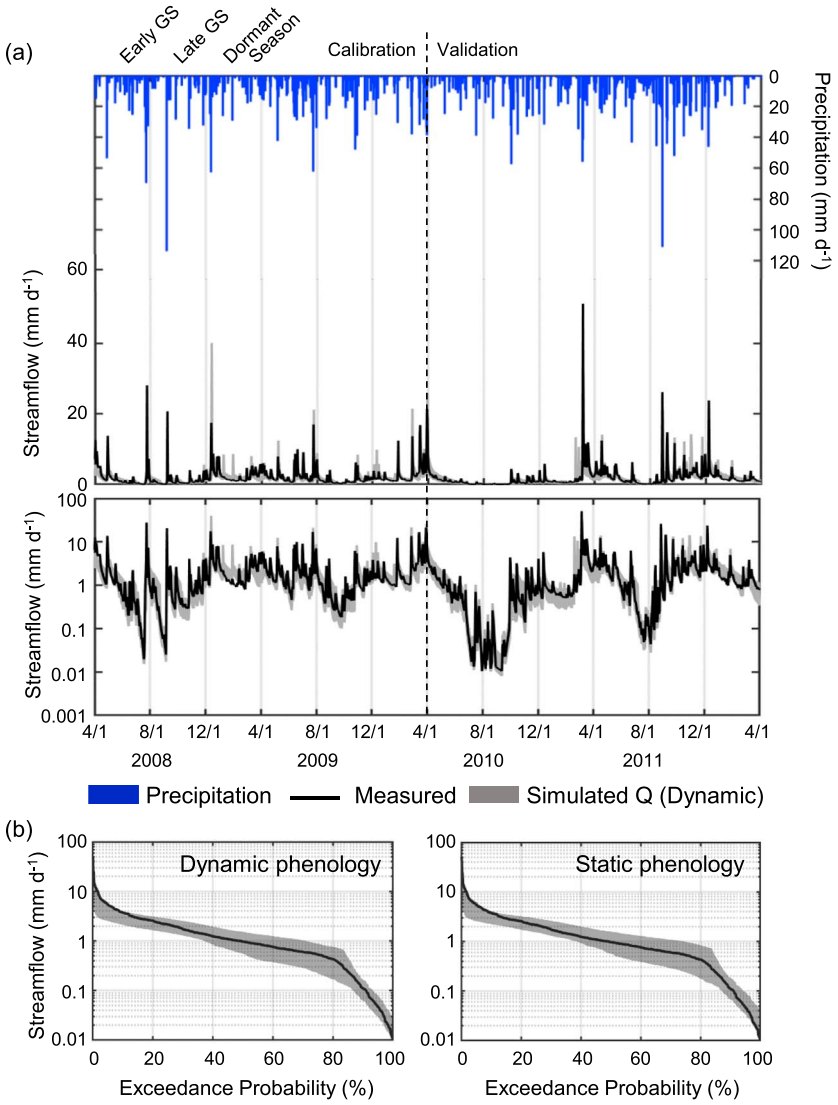

Figure 5. (a) Simulated (grey area) and measured (black line) daily catchment discharge (*Q*) of the study catchment under the dynamic phenology scheme (linear-scale on top; log-scale on bottom). The grey areas represent 95% confidence intervals from the behavior model runs (n = 146). (b) Exceedance probabilities (%) of the simulated *Q* under the dynamic and static phenology scheme, respectively (grey area), and that of the measured *Q* (black line).

Table 1
The Performance Measures of the Catchment Discharge Simulation Under the Dynamic and Static Phenology Schemes During the Validation Period (May 2010 to April 2012)

Phenology scheme	NSE	NSE_{log}	RMSE	PBIAS
Dynamic	0.423	0.644	0.97	16.2%
Static	0.381	0.632	0.98	16.5%

Note. Three measures (NSE: Nash-Sutcliffe efficiency, NSE_{log}: Nash-Sutcliffe efficiency for log-stream discharge, RMSE: the root-mean-squared-error, and PBIAS: percent bias) indicate that the model performed better with the dynamic phenology scheme. Note that these are the median values of the behavioral model runs (n = 146).

In addition to the plot-scale variables, the model also showed good performance in simulating the catchment discharge (Figure 5; 146 behavioral model runs). The model (dynamic phenology) generally simulated low flows better (NSE_{log} = 0.692 and 0.644 for calibration and validation, respectively; Table 1) than for high flows (NSE = 0.461 and 0.423), which may be partially due to the somewhat inaccurate simulations in snow accumulation and melt timing in the springs of 2009 and 2011 (Figure 5a). The RMSE for the daily discharge was less than 1 mm for both calibration and validation periods (0.91 and 0.97 mm, respectively; PBIAS of 11.6% and 16.2%). Even without further calibrations, the measured data were matched with the simulated daily discharge slightly better under the dynamic phenology scheme than under the static phenology scheme (NSE_{log} = 0.671 and 0.632;

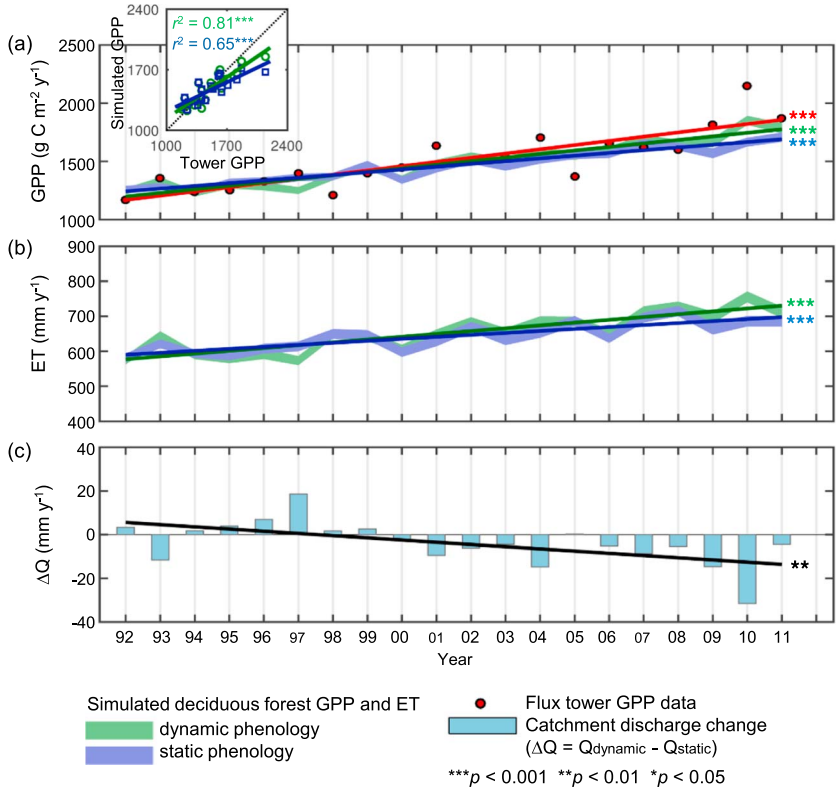

Figure 6. (a and b) Simulated annual gross primary productivity (GPP) and evapotranspiration (ET) of the deciduous forest under the dynamic and static phenology schemes (green and blue areas, respectively) and their long-term trends (solid lines in each color and significance in asterisk). Each area represents 95% confidence intervals from the behavioral model runs (n = 146). The gap-filled tower GPP data were compared to the simulated GPP under the two phenology schemes (a-insert). (c) Change in the catchment discharge due to the phenological changes (ΔQ in bar) and its long-term trend over the 20-year study period (light blue solid line, significance values indicated with asterisks).

NSE = 0.453 and 0.381; RMSE = 0.91 and 0.98 mm/day; PBIAS = 11.9% and 16.5% for calibration and validation, respectively; Table 1 and Figure 5b).

3.3. Implications of the Phenological Changes

The simulated annual GPP and ET of the deciduous forest significantly increased over the study period, which were mostly attributed to climate forcing and vegetation response to it (i.e., under the static phenology scheme; 235.2 g C/m^2 and 57 mm increases per decade, 18.8% and 9.5% increases, respectively; both $p < 0.001$; Figures 6a and 6b). However, the increasing rate of the simulated GPP was much smaller than that of the tower-based estimates (361.3 g C/m^2 per decade, 28.9%). When the dynamic phenology scheme was integrated, not only were the rate comparisons better (303.2 g C/m^2 and 81 mm increases per decade, 24.2% and 13.5% increases, respectively; both $p < 0.001$), but the interannual variation was also better accounted for (r^2 = 0.81 and 0.65 under the dynamic and static phenology schemes, respectively; inset of Figure 6a). Meanwhile, for the evergreen forest, the simulated annual GPP and ET increased by 218.3 g C/m^2 and 85 mm per decade (21.8% and 17.1% increases, respectively; $p < 0.001$). Within our unified modeling framework, the phenological changes of the deciduous forest reduced the catchment annual discharge by 6.1 mm per decade as compared to that estimated with the static phenology scheme ($p < 0.01$; Figure 6c).

The greenup and senescence onset variations appeared to have asymmetrical effects on the interannual flux changes revealed by our model results (Figure 7). The greenup variation significantly affected the annual GPP and ET as well as the catchment discharge, whereas the senescence onset variations induced little change. Earlier greenup onset significantly increased GPP by 10.6 g C/m^2 per day ($r = -0.93$, $p < 0.001$) as well as ET by 3.9 mm ($r = -0.94$, $p < 0.001$), while catchment discharge was decreased by 1.1 mm (r = 0.92,

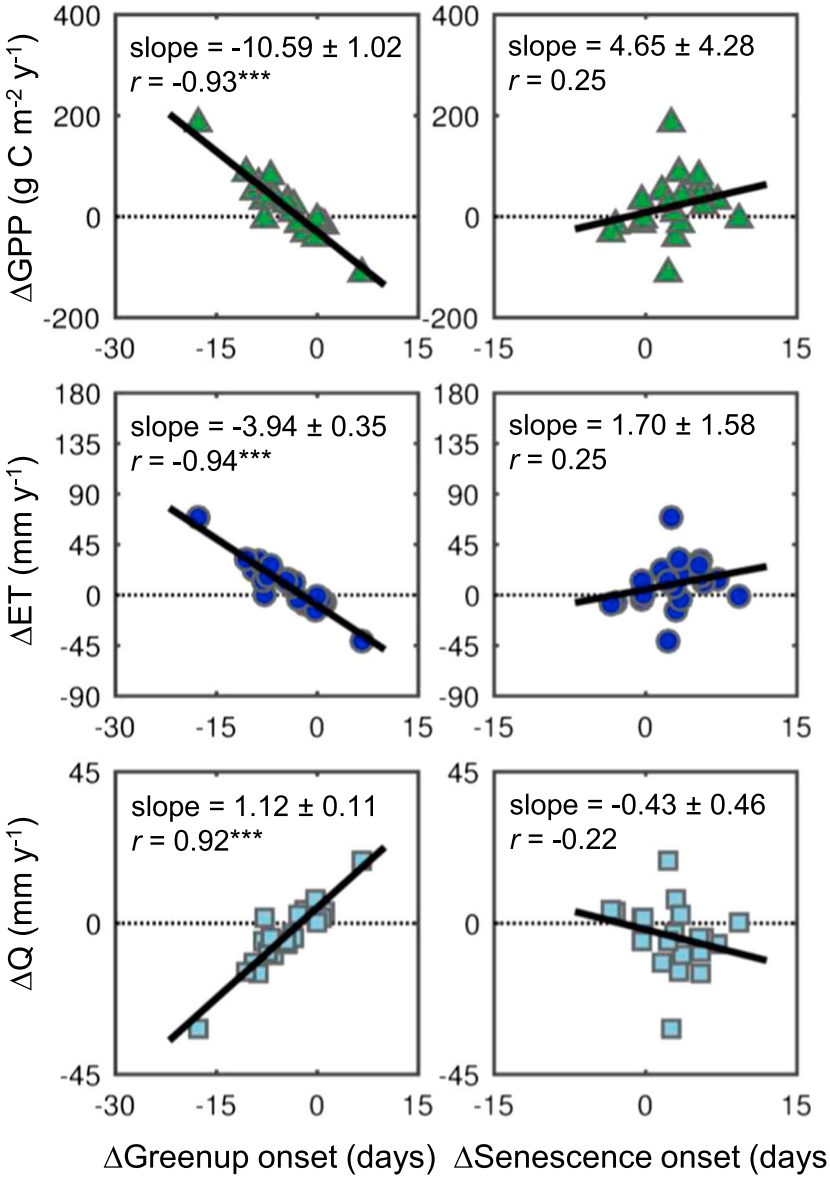

Figure 7. Net effects of greenup and senescence variations on changes in the annual GPP and ET changes of the deciduous forest (ΔGPP and ΔET) and in the annual catchment discharge (Δ*Q*). ΔGPP, ΔET, and Δ*Q* are the differences between the dynamic (the interannually variable greenup and senescence timings) and static (fixed greenup and senescence timings from 1992) phenology schemes under the same climatic conditions. A linear least squares regression was applied to estimate the best relationship (solid line) with the slope, correlation coefficient (*r*), and significance shown ($^{***}p < 0.001$, $^{**}p < 0.01$, $^{*}p < 0.05$).

$p < 0.001$). Later senescence onset displayed similar effects (i.e., increases in GPP and ET and a decrease in the catchment discharge), but the magnitude was about half and not significant ($p > 0.05$).

Within our modeling framework, the effect of the variations in the greenup onset of the deciduous forest on the ET and the catchment discharge varied between seasons (Figure 8). Earlier greenup onset significantly increased the ET during the early GS (April–July) by 3.9 mm per day ($r = -0.97$, $p < 0.001$), while decreasing catchment discharge by 0.7 mm ($r = 0.74$, $p < 0.001$). On the other hand, during the late GS (August–November), the greenup variation had weak and not significant effects on both the ET and catchment discharge ($p > 0.05$). Interestingly, during the following dormant season (December–March), the changes in catchment discharge (Δ*Q*) was again significantly correlated with the greenup onset variation, with a

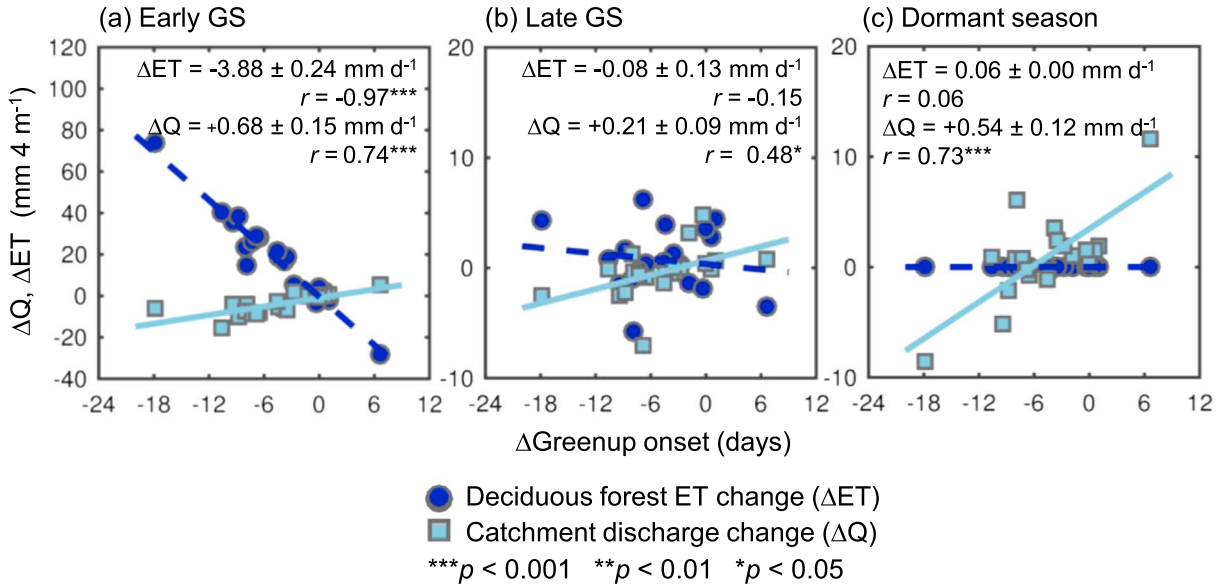

Figure 8. Net effects of greenup variations on the changes in the deciduous forest ET (ΔET, blue circle) and the catchment discharge (Δ*Q*, light blue square) during (a) early growing season (GS; April to July), (b) late GS (august to November), and (c) following dormant season (December to March). The ΔET and Δ*Q* are the differences between the dynamic and static phenology schemes under the same climatic condition.

decrease of 0.5 mm per earlier greenup onset day ($r = 0.73$, $p < 0.001$). The variations in the senescence onset were not correlated with any of the flux changes above ($p > 0.05$; not shown here).

4. Discussion

In this study, we examined the net effect of phenological changes on the long-term and interannual carbon and water fluxes (GPP and ET) in a temperate deciduous forest and scaled the plot-scale dynamics up to the catchment-scale stream discharge behavior at a mixed deciduous-conifer study watershed (Figure 1). We integrated spring and autumn phenology models into the mechanistic watershed ecohydrological model and separated the dominant climatic controls by implementing the model under the "static" and "dynamic" phenology schemes. During the study period (1992–2011), the onsets of greenup and senescence were significantly advanced and delayed, respectively (Figure 2). The daily simulations at both the plot (GPP, ET, LAI, and soil respiration) and catchment (stream discharge) scales were improved once the dynamic phenology was incorporated, as compared to results under the static phenology scheme (Figures 3–6, Table 1, and Figures S4 and S5). The phenological changes accounted for both long-term and interannual variations in the annual GPP and ET (Figure 6). In particular, earlier greenup onset was significantly correlated with interannual variations in GPP and ET, while delayed senescence onset had little influence (Figure 7). At the catchment scale, earlier greenup onset reduced stream discharge not only during the GS but also throughout the following dormant season (Figure 8).

Our results show that the warming-induced phenological variations have amplified the long-term trends in the GPP and ET driven by climatic controls. The daily ET increased promptly along with the greenup onset (Figure 4) because soil water is usually plentiful after the recharge during dormant season at the study site (Urbanski et al., 2007). The enhanced vegetation water use during the early GS led to higher soil water depletion (i.e., lower water table depth during the late GS in Figure S6), therefore reducing catchment discharge throughout the GS (Figures 8a and 8b). However, the late GS ET was not suppressed by the increased soil water depletion (i.e., little correlation with the greenup onset variation), but rather increased (Figure 8b). This suggests that the stomatal conductance was not strongly constrained by soil moisture even toward the end of GS, either because it rarely dropped below critical value or the water table was shallow enough that trees with deep roots can access it (Urbanski et al., 2007). The increases in the late GS ET might be accounted for the enhanced photosynthesis and subsequent increases in LAI by earlier greenup onset, known as "a positive lagged effect" (Richardson et al., 2010). For instance, greenup onset 18 days earlier in

2010 led to a 0.38 higher GS LAI than the LAI under a static phenology scheme, which was accompanied by an increase in the late GS ET by 3.92 mm, where senescence onset delay by 2.6 days could only account for 0.92 mm ($p > 0.05$; Figure 7). Meanwhile, an extended canopy duration by the delayed senescence had little influence on the annual GPP and ET, as well as the catchment discharge in general. This might be attributed to other constraints, such as temperature or photoperiod, exerting dominant controls on photosynthetic activity at this time of year (Barichivich et al., 2013; Bauerle et al., 2012; Urbanski et al., 2007). This would lead to decoupling of the canopy duration and the stomatal dynamics, resulting in the asymmetric flux profiles between the early and late GS. Note that strong photoperiod regulation during the late GS was also captured in the phenology model calibration. The autumn phenology model with DOY (i.e., day length) showed a higher accuracy than the one with temperature, while the spring phenology model was opposite (Figure S2).

The importance of phenological controls on the watershed-scale hydrologic behavior has long been suggested by several studies (Richardson et al., 2013; Thompson et al., 2011), but, to date, few studies have assessed its net effect within a unified modeling framework using both plot- and catchment-scale data. In this study, we showed that integrating dynamic phenology improved the simulation results not only at the plot-scale but also for catchment-scale discharge dynamics. Both high and low flows were better simulated once dynamic phenology was incorporated, and enhanced vegetation water use during the GS resulted in lower stream discharge throughout the following dormant season. Our study also showed that the effect of the phenological variations on catchment discharge was damped relative to its effect on the plot-scale ET due to the mixed deciduous-conifer forest cover in this study catchment. This implies that changes in stream discharge might be quite different between watersheds depending on the forest compositions and lateral interactions within each watershed.

The role of vegetation dynamics on the hydrological regime changes in the eastern United States has been discussed by both hydrology and terrestrial ecology communities (Huntington, 2010; Huntington et al., 2004; Richardson et al., 2013). However, these effects, especially at a seasonal scale, are also greatly affected by a wide variation in short- and long-term hydroclimate variability and their transient effects on soil moisture dynamics (Nippgen et al., 2016). After separating the effects of climatic variation from those of phenology within the unified modeling framework, the variation in greenup onset appears to have a lagged effect on the watershed discharge, not just during the GS but throughout the year with a different magnitude each season. The stream discharge reduces most with earlier greenup onset during the early GS periods and least during the following dry periods (i.e., the late GS). The effect of increased soil water depletion during the GS on streamflow dynamics was carried over throughout the following dormant season, often referred as a "*memory effect*" of watershed systems (Nippgen et al., 2016; Scaife & Band, 2017). The earlier greenup onset in 2010 (by 18 days) resulted in lower water table depth by 200 mm (12.9%; Figure S6). This study therefore suggests that greenup onset can be an effective diagnostic of hydrologic regime changes, especially in deciduous forests in this region.

It is worthwhile to note that not all watersheds would have clear links between GS dynamics and carbon/water fluxes. In the eastern United States, precipitation is relatively evenly distributed throughout a year, and shallow soil moisture is a primary source for both ET and surface runoff in forested watersheds (Hewlett & Hibbert, 1963). These abiotic factors may have resulted in tight coupling between GS dynamics and associated hydrological processes as shown this study. However, such transient responses of streamflow to GS dynamics may be prevailed in the watersheds where deep groundwater flow is the dominant runoff generation mechanism (Tague, 2009; Tague et al., 2008) or where subsurface flows are seasonally decoupled with vegetation water use (i.e., transpiration) due to a seasonally dry climate (Renée Brooks et al., 2010). In water-limited ecosystems, in particular, several studies reported that a positive lagged effect of earlier greenup onset on carbon uptake (therefore presumably ET as well) during the early GS can be diminished or even offset by the increased soil water deficit toward the late GS (Angert et al., 2005; Hu et al., 2010; White & Nemani, 2003; Yu et al., 2018). This suggests that stomatal response to drought stress would also decouple canopy duration dynamics with vegetation carbon uptake and its water use as well as with the watershed stream discharge in an annual-scale.

Our results suggest that warming-induced earlier greenup onsets may have partially mitigated the ongoing increases in stream discharge in the northeastern United States, which have been mainly attributed to the warming-induced changes in precipitation patterns (e.g., intense rainfalls and increased amount;

Huntington & Billmire, 2014; Weider & Boutt, 2010). Given that the advance in the greenup onset is expected to continue with the ongoing climate change (Migliavacca et al., 2012; Richardson et al., 2013), the projected higher streamflow in winter and spring (Hayhoe et al., 2007) may in part be lessened by increased soil water depletion inherited from earlier greenup onsets in the previous GS. For a better prediction of future hydrologic regime changes in the region, it is important to improve our understanding of the hydrologic nonstationarity attributed to the phenological changes at both seasonal and decadal time scales.

5. Conclusion

In this study, we separated the phenological and climatic controls within a unified ecohydrological modeling framework and assessed the net effects of earlier greenup and delayed senescence onsets on the GPP and ET of a deciduous forest, as well as on the stream discharge of the larger mixed-forest catchment, in the northeastern United States. We showed that the long-term increases in the annual GPP and ET of the deciduous forest have been amplified due to the phenological changes over the last two decades. Earlier greenup onsets have significantly reduced the catchment discharge, which persists through the following dormant season due to inherited soil water depletion from the previous GSs. However, senescence onset variations were not found to be a significant factor of the interannual variations in those fluxes.

Recent global-scale remote sensing data sets (e.g., GIMMS NDVI3g and MODIS) now provide unique opportunities to effectively monitor vegetation phenological changes across different regions, in which emergent changes in the watershed-scale hydrologic behavior may be accounted for by the vegetation dynamics (Hwang et al., 2018). The nonstationary behavior of watersheds may have a great impact on the generation of the surface water, which serves as primary sources of clean freshwater to adjacent urban areas, for example, in the eastern United States. Given the ongoing changes in vegetation phenology and its consequent effect on the carbon and water cycle dynamics, further research is needed to predict the changes in the amount and timing of freshwater yield and accompanying nutrient exports in those regions. Our study highlights the need for improvements in our understanding of the terrestrial ecosystem response to changing climate and clarification of its feedback effect on long-term and seasonal hydrologic regime changes.

Acknowledgments

This study was supported in part by the NASA MODIS science team (grant NNX11AD58G), the NASA Carbon Science program (grant NNX17AE69G), and the USGS Science Team (grant ING12PC00072). The Harvard Forest EMS flux tower has been supported by the Office of Science (BER) at the U.S. Department of Energy (DOE) under various subprograms over the years, and this tower is now a core site in AmeriFlux network (grant DE-AC02-05CH11231). The long-term meteorological and hydrological measurements at Harvard Forest are also supported through the National Science Foundation Long-Term Ecological Research Program (grant NSF-DEB-1237491). All data sets used in this study are available to download in the links below.

1. Climate data (daily temperature and precipitation; Figure 5)
   Shaler station
   http://harvardforest.fas.harvard.edu/data/p00/hf000/hf000-01-daily-m.csv
   Fisher station
   http://harvardforest.fas.harvard.edu/data/p00/hf001/hf001-06-daily-m.csv

References

Angert, A., Biraud, S., Bonfils, C., Henning, C. C., Buermann, W., Pinzon, J., et al. (2005). Drier summers cancel out the CO_2 uptake enhancement induced by warmer springs. *Proceedings of the National Academy of Sciences of the United States of America*, *102*(31), 10,823–10,827. https://doi.org/10.1073/pnas.0501647102

Baldocchi, D. D. (2008). "Breathing" of the terrestrial biosphere: Lessons learned from a global network of carbon dioxide flux measurement systems. *Australian Journal of Botany*, *56*(1), 1. https://doi.org/10.1071/BT07151

Band, L. E., Tague, C. L., Groffman, P. M., & Belt, K. (2001). Forest ecosystem processes at the watershed scale: Hydrological and ecological controls of nitrogen export. *Hydrological Processes*, *15*(10), 2013–2028. https://doi.org/10.1002/hyp.253

Barford, C. C. (2001). Factors controlling long- and short-term sequestration of atmospheric CO_2 in a mid-latitude forest. *Science*, *294*(5547), 1688–1691. https://doi.org/10.1126/science.1062962

Barichivich, J., Briffa, K. R., Myneni, R. B., Osborn, T. J., Melvin, T. M., Ciais, P., et al. (2013). Large-scale variations in the vegetation growing season and annual cycle of atmospheric CO_2 at high northern latitudes from 1950 to 2011. *Global Change Biology*, *19*(10), 3167–3183. https://doi.org/10.1111/gcb.12283

Bauerle, W. L., Oren, R., Way, D. A., Qian, S. S., Stoy, P. C., Thornton, P. E., et al. (2012). Photoperiodic regulation of the seasonal pattern of photosynthetic capacity and the implications for carbon cycling. *Proceedings of the National Academy of Sciences of the United States of America*, *109*(22), 8612–8617. https://doi.org/10.1073/pnas.1119131109

Berry, J. A., Beerling, D. J., & Franks, P. J. (2010). Stomata: Key players in the earth system, past and present. *Current Opinion in Plant Biology*, *13*(3), 232–239. https://doi.org/10.1016/j.pbi.2010.04.013

Beven, K. J., & Binley, A. (1992). The future of distributed models: Model calibration and uncertainty prediction. *Hydrological Processes*, *6*(3), 279–298. https://doi.org/10.1002/hyp.3360060305

Boose, E. (2018a). Fisher Meteorological Station at Harvard Forest since 2001. Harvard Forest Data Archive: HF001. https://doi.org/10.6073/pasta/04076dfd30b286c6c29301b6345a63f5

Boose, E. (2018b). Prospect Hill Hydrological Stations at Harvard Forest since 2005. Harvard Forest Data Archive: HF070. https://doi.org/10.6073/pasta/56496bd0ff0073ccfd76474a42f6ac45

Boose, E., & Gould, E. (2004). Shaler Meteorological Station at Harvard Forest 1964-2002. Harvard Forest Data Archive: HF000. https://doi.org/10.6073/pasta/84cf303ea3331fb47e8791aa61aa91b2

Buitenwerf, R., Rose, L., & Higgins, S. I. (2015). Three decades of multi-dimensional change in global leaf phenology. *Nature Climate Change*, 1–5. https://doi.org/10.1038/nclimate2533

Christensen, L., Tague, C. L., & Baron, J. S. (2008). Spatial patterns of simulated transpiration response to climate variability in a snow dominated mountain ecosystem. *Hydrological Processes*, *22*(18), 3576–3588. https://doi.org/10.1002/hyp.6961

Churkina, G., Schimel, D., Braswell, B. H., & Xiao, X. (2005). Spatial analysis of growing season length control over net ecosystem exchange. *Global Change Biology*, *11*(10), 1777–1787. https://doi.org/10.1111/j.1365-2486.2005.001012.x

2. Leaf observation (size and coloration) data (Figures S1 and S2)
   http://harvardforest.fas.harvard.edu/data/p00/hf003/hf003-03-spring.csv
   http://harvardforest.fas.harvard.edu/data/p00/hf003/hf003-04-fall.csv
3. Stream discharge data (Figure 5)
   http://harvardforest.fas.harvard.edu/data/p07/hf070/hf070-03-daily.csv
4. Flux tower data (GPP, ET, atmospheric CO_2 concentration, vapor pressure deficit, wind speed, and photosynthetically active radiation)
   EMS tower (Figures 3a, 4a, and 6a)
   http://harvardforest.fas.harvard.edu/data/p00/hf004/hf004-01-final.csv
   http://harvardforest.fas.harvard.edu/data/p00/hf004/hf004-02-filled.csv
   HEM tower (Figure S3a)
   http://harvardforest.fas.harvard.edu/data/p10/hf103/hf103-03-flux-2004-2013.csv
5. Ground-measured data (LAI and soil respiration)
   Deciduous forest (Figures S4a and S5a)
   http://harvardforest.fas.harvard.edu/data/p00/hf006/hf006-01-soil-respiration.csv
   http://harvardforest.fas.harvard.edu/data/p06/hf069/hf069-02-LAI-site.csv
   http://harvardforest.fas.harvard.edu/data/p06/hf069/hf069-08-soil.resp.csv
   http://harvardforest.fas.harvard.edu/data/p06/hf069/hf069-17-allometries.txt
   Coniferous forest (Figures S4c and S5b)
   http://harvardforest.fas.harvard.edu/data/p15/hf150/hf150-01-hem-lai.csv
   http://harvardforest.fas.harvard.edu/data/p14/hf148/hf148-01-hem-soil-respiration.csv
6. LiDAR bare-earth surface model
   https://docs.digital.mass.gov/dataset/massgis-data-lidar-terrain-data
7. Aerial photo in April 2009 (Figure 1)
   https://www.mass.gov/anf/research-and-tech/it-serv-and-support/application-serv/office-of-geographic-information-massgis/datalayers/colororthos2008.html
8. Wetland boundary (Figure 1)
   http://harvardforest.fas.harvard.edu/data/p11/hf110/hf110-01-gis.zip
9. RHESSys model
   Source code: https://github.com/RHESSys/RHESSys

Cohen, W. B., Turner, D. P., Gower, S. T., & Running, S. W. (2006). BigFoot land cover surfaces for North and South American sites, 2000–2003. Data set. Available on-line [http://www.daac.ornl.gov] from Oak RidgeNational Laboratory Distributed Active Archive Center, Oak Ridge, Tennessee, U.S.A.

Creed, I. F., Hwang, T., Lutz, B., & Way, D. (2015). Climate warming causes intensification of the hydrological cycle, resulting in changes to the vernal and autumnal windows in a northern temperate forest. *Hydrological Processes*, *29*(16), 3519–3534. https://doi.org/10.1002/hyp.10450

Creed, I. F., Spargo, A. T., Jones, J. A., Buttle, J. M., Adams, M. B., Beall, F. D., et al. (2014). Changing forest water yields in response to climate warming: results from long-term experimental watershed sites across North America. *Global Change Biology*, *20*(10), 3191–3208. https://doi.org/10.1111/gcb.12615

Czikowsky, M. J., & Fitzjarrald, D. R. (2004). Evidence of seasonal changes in evapotranspiration in eastern U.S. hydrological records. *Journal of Hydrometeorology*, *5*(5), 974–988. https://doi.org/10.1175/1525-7541(2004)005<0974:EOSCIE>2.0.CO;2

Dingman, S. L. (2009). *Physical hydrology* (2nd ed.). Long Grove, Illinois: Waveland Press.

Elmore, A. J., Nelson, D. M., & Craine, J. M. (2016). Earlier springs are causing reduced nitrogen availability in North American eastern deciduous forests. *Nature Plants*, *2*(10), 1–5. https://doi.org/10.1038/nplants.2016.133

Foster, D., & Boose, E. (1999). Historical GIS data for Harvard Forest properties from 1908 to present. Harvard Forest data archive: HF110. https://doi.org/10.6073/pasta/3f7847c8bc91547fffec4d69079516c4

Hadley, J. L., Kuzeja, P. S., Daley, M. J., Phillips, N. G., Mulcahy, T., & Singh, S. (2008). Water use and carbon exchange of red oak- and eastern hemlock-dominated forests in the northeastern USA: Implications for ecosystem-level effects of hemlock woolly adelgid. *Tree Physiology*, *28*(4), 615–627. https://doi.org/10.1093/treephys/28.4.615

Hayhoe, K., Wake, C. P., Huntington, T. G., Luo, L., Schwartz, M. D., Sheffield, J., et al. (2007). Past and future changes in climate and hydrological indicators in the US Northeast. *Climate Dynamics*, *28*(4), 381–407. https://doi.org/10.1007/s00382-006-0187-8

Hewlett, J. D., & Hibbert, A. R. (1963). Moisture and energy conditions within a sloping soil mass during drainage. *Journal of Geophysical Research*, *68*(4), 1081–1087. https://doi.org/10.1029/JZ068i004p01081

Hogg, E. H., Price, D. T., & Black, T. A. (2000). Postulated feedbacks of deciduous forest phenology on seasonal climate patterns in the western Canadian interior. *Journal of Climate*, *13*(24), 4229–4243. https://doi.org/10.1175/1520-0442(2000)013<4229:PFODFP>2.0.CO;2

Hu, J., Moore, D. J. P., Burns, S. P., & Monson, R. (2010). Longer growing seasons lead to less carbon sequestration by a subalpine forest. *Global Change Biology*, *16*(2), 771–783. https://doi.org/10.1111/j.1365-2486.2009.01967.x

Huntington, T. G. (2010). Climate warming-induced intensification of the hydrologic cycle. In *Advances in Agronomy* (Vol. 109, pp. 1–53). Cambridge, MA: Elsevier. https://doi.org/10.1016/B978-0-12-385040-9.00001-3

Huntington, T. G., & Billmire, M. (2014). Trends in precipitation, runoff, and evapotranspiration for rivers draining to the Gulf of Maine in the United States. *Journal of Hydrometeorology*, *15*(2), 726–743. https://doi.org/10.1175/JHM-D-13-018.1

Huntington, T. G., Survey, U. S. G., & Rd, W. (2004). Climate change, growing season length, and transpiration: Plant response could alter hydrologic regime. *Plant Biology*, *6*(6), 651–653. https://doi.org/10.1055/s-2004-830353

Hwang, T., Band, L. E., & Hales, T. C. (2009). Ecosystem processes at the watershed scale: Extending optimality theory from plot to catchment. *Water Resources Research*, *45*, W11425. https://doi.org/10.1029/2009WR007775

Hwang, T., Band, L. E., Miniat, C. F., Song, C., Bolstad, P. V., Vose, J. M., & Love, J. P. (2014). Divergent phenological response to hydroclimate variability in forested mountain watersheds. *Global Change Biology*, *20*(8), 2580–2595. https://doi.org/10.1111/gcb.12556

Hwang, T., Kang, S., Kim, J., Kim, Y., Lee, D., & Band, L. E. (2008). Evaluating drought effect on MODIS gross primary production (GPP) with an eco-hydrological model in the mountainous forest, East Asia. *Global Change Biology*, *14*(5), 1037–1056. https://doi.org/10.1111/j.1365-2486.2008.01556.x

Hwang, T., Martin, K. L., Vose, J. M., Wear, D., Miles, B., & Band, L. E. (2018). Non-stationary hydrologic behavior in forested watersheds is mediated by climate-induced changes in growing season length and subsequent vegetation growth. *Water Resources Management*. https://doi.org/10.1029/2017WR022279

Hwang, T., Song, C., Bolstad, P. V., & Band, L. E. (2011). Downscaling real-time vegetation dynamics by fusing multi-temporal MODIS and Landsat NDVI in topographically complex terrain. *Remote Sensing of Environment*, *115*(10), 2499–2512. https://doi.org/10.1016/j.rse.2011.05.010

Hwang, T., Song, C., Vose, J. M., & Band, L. E. (2011). Topography-mediated controls on local vegetation phenology estimated from MODIS vegetation index. *Landscape Ecology*, *26*(4), 541–556. https://doi.org/10.1007/s10980-011-9580-8

Jones, J. A., Creed, I. F., Hatcher, K. L., Warren, R. J., Adams, M. B., Melinda, H., et al. (2012). Ecosystem processes and human influences regulate streamflow response to climate change at long-term ecological research sites. *Bioscience*, *62*(4), 390–404. https://doi.org/10.1525/bio.2012.62.4.10

Keeling, C. D., Chin, J. F. S., & Whorf, T. P. (1996). Increased activity of northern vegetation inferred from atmospheric CO_2 measurements. *Nature*, *382*(6587), 146–149. https://doi.org/10.1038/382146a0

Keenan, T. F., Gray, J., Friedl, M. A., Toomey, M., Bohrer, G., Hollinger, D. Y., et al. (2014). Net carbon uptake has increased through warming-induced changes in temperate forest phenology. *Nature Climate Change*, *4*(7), 598–604. https://doi.org/10.1038/nclimate2253

Keenan, T. F., Hollinger, D. Y., Bohrer, G., Dragoni, D., Munger, J. W., Schmid, H. P., & Richardson, A. D. (2013). Increase in forest water-use efficiency as atmospheric carbon dioxide concentrations rise. *Nature*, *499*(7458), 324–327. https://doi.org/10.1038/nature12291

Kelly, C. N., McGuire, K. J., Miniat, C. F., & Vose, J. M. (2016). Streamflow response to increasing precipitation extremes altered by forest management. *Geophysical Research Letters*, *43*, 3727–3736. https://doi.org/10.1002/2016GL068058

Kim, J., Hwang, T., Schaaf, C. L., Orwig, D. A., Boose, E., & Munger, J. W. (2017). Increased water yield due to the hemlock woolly adelgid infestation in New England. *Geophysical Research Letters*, *44*, 2327–2335. https://doi.org/10.1002/2016GL072327

Kramer, R., Bounoua, L., Zhang, P., Wolfe, R., Huntington, T. G., Imhoff, M., et al. (2015). Evapotranspiration trends over the eastern United States during the 20th century. *Hydrology*, *2*(2), 93–111. https://doi.org/10.3390/hydrology2020093

Lin, L., Webster, J. R., Hwang, T., & Band, L. E. (2015). Effects of lateral nitrate flux and instream processes on dissolved inorganic nitrogen export in a forested catchment: A model sensitivity analysis. *Water Resources Research*, *51*, 2680–2695. https://doi.org/10.1002/2014WR015962

Loescher, H. W., Gholz, H. L., Jacobs, J. M., & Oberbauer, S. F. (2005). Energy dynamics and modeled evapotranspiration from a wet tropical forest in Costa Rica. *Journal of Hydrology*, *315*(1-4), 274–294. https://doi.org/10.1016/j.jhydrol.2005.03.040

Lu, H., Bryant, R. B., Buda, A. R., Collick, A. S., Folmar, G. J., & Kleinman, P. J. A. (2015). Long-term trends in climate and hydrology in an agricultural, headwater watershed of central Pennsylvania, USA. *Journal of Hydrology: Regional Studies*, *4*, 713–731. https://doi.org/10.1016/j.ejrh.2015.10.004

Menzel, A., Sparks, T. H., Estrella, N., Koch, E., Aasa, A., Ahas, R., et al. (2006). European phenological response to climate change matches the warming pattern. *Global Change Biology*, *12*(10), 1969–1976. https://doi.org/10.1111/j.1365-2486.2006.01193.x

Migliavacca, M., Sonnentag, O., Keenan, T. F., Cescatti, A., O'Keefe, J., & Richardson, A. D. (2012). On the uncertainty of phenological responses to climate change, and implications for a terrestrial biosphere model. *Biogeosciences*, *9*(6), 2063–2083. https://doi.org/10.5194/bg-9-2063-2012

Munger, J. W., & Hadley, J. L. (2017). Net carbon exchange of an old-growth hemlock forest at Harvard Forest HEM Tower since 2000. Harvard Forest Data Archive: HF103. https://doi.org/10.6073/pasta/eae9d5adcea3afc30e94c20e6b710a22

Munger, J. W., & Wofsy, S. C. (2017). Canopy-atmosphere exchange of carbon, water and energy at Harvard Forest EMS Tower since 1991. Harvard Forest Data Archive: HF004. https://doi.org/10.6073/pasta/dd9351a3ab5316c844848c3505a8149d

Munger, J. W., & Wofsy, S. C. (2018). Biomass inventories at Harvard Forest EMS Tower since 1993. Harvard Forest Data Archive: HF069. https://doi.org/10.6073/pasta/37ff12d47894a73ddd9d86c1225e2dc8

Nash, J. E., & Sutcliffe, J. V. (1970). River flow forecasting through conceptual models. Part I—A discussion of principles. *Journal of Hydrology*, *10*(3), 282–290. https://doi.org/10.1016/0022-1694(70)90255-6

Nippgen, F., McGlynn, B. L., Emanuel, R. E., & Vose, J. M. (2016). Watershed memory at the Coweeta Hydrologic Laboratory: The effect of past precipitation and storage on hydrologic response. *Water Resources Research*, *52*, 1673–1695. https://doi.org/10.1002/2015WR018196

NRCS. (2009). Soil Survey Geographic (SSURGO) Database USDA NRCS [National Resources Conservation Service]. Retrieved from http://sdmdataaccess.nrcs.usda.gov/, Accessed Mar/30/2012.

O'Keefe, J. (2015). Phenology of woody species at Harvard Forest since 1990. Harvard Forest Data Archive: HF003. https://doi.org/10.6073/pasta/a32b4030903b86b43a1a3d4157a0fcf3

Parton, W. J., Mosier, A. R., Ojima, D., Valentine, D. W., Schimel, D. S., Weier, K., & Kulmala, A. E. (1996). Generalized model for N_2 and N_2O production from nitrification and denitrification. *Global Biogeochemical Cycles*, *10*(3), 401–412. https://doi.org/10.1029/96GB01455

Parton, W. J., Scurlock, J. M. O., Ojima, D., Gilmanov, T. G., Scholes, R. J., Schimel, D. S., et al. (1993). Observations and modeling of biomass and soil organic matter dynamics for the grassland biome worldwide. *Global Biogeochemical Cycles*, *7*(4), 785–809. https://doi.org/10.1029/93GB02042

Patric, J. H., & Reinhart, K. G. (1971). Hydrologic effects of deforesting two mountain watersheds in West Virginia. *Water Resources Research*, *7*(5), 1182–1188. https://doi.org/10.1029/WR007i005p01182

Penuelas, J., Rutishauser, T., & Filella, I. (2009). Phenology feedbacks on climate change. *Science*, *324*(5929), 887–888. https://doi.org/10.1126/science.1173004

Polgar, C. A., & Primack, R. B. (2011). Leaf-out phenology of temperate woody plants: From trees to ecosystems. *New Phytologist*, *191*(4), 926–941. https://doi.org/10.1111/j.1469-8137.2011.03803.x

Puma, M. J., Koster, R. D., & Cook, B. I. (2013). Phenological versus meteorological controls on land-atmosphere water and carbon fluxes. *Journal of Geophysical Research: Biogeosciences*, *118*, 14–29. https://doi.org/10.1029/2012JG002088

Renée Brooks, J., Barnard, H. R., Coulombe, R., & McDonnell, J. J. (2010). Ecohydrologic separation of water between trees and streams in a Mediterranean climate. *Nature Geoscience*, *3*(2), 100–104. https://doi.org/10.1038/ngeo722

Richardson, A. D., Anderson, R. S., Arain, M. A., Barr, A. G., Bohrer, G., Chen, G., et al. (2012). Terrestrial biosphere models need better representation of vegetation phenology: Results from the North American Carbon Program Site Synthesis. *Global Change Biology*, *18*(2), 566–584. https://doi.org/10.1111/j.1365-2486.2011.02562.x

Richardson, A. D., Andy Black, T., Ciais, P., Delbart, N., Friedl, M. A., Gobron, N., et al. (2010). Influence of spring and autumn phenological transitions on forest ecosystem productivity. *Philosophical Transactions of the Royal Society, B: Biological Sciences*, *365*(1555), 3227–3246. https://doi.org/10.1098/rstb.2010.0102

Richardson, A. D., Bailey, A. S., Denny, E. G., Martin, C. W., & O'Keefe, J. (2006). Phenology of a northern hardwood forest canopy. *Global Change Biology*, *12*(7), 1174–1188. https://doi.org/10.1111/j.1365-2486.2006.01164.x

Richardson, A. D., Hollinger, D. Y., Dail, D. B., Lee, J. T., Munger, J. W., O'Keefe, J., & O'keefe, J. (2009). Influence of spring phenology on seasonal and annual carbon balance in two contrasting New England forests. *Tree Physiology*, *29*(3), 321–331. https://doi.org/10.1093/treephys/tpn040

Richardson, A. D., Keenan, T. F., Migliavacca, M., Ryu, Y., Sonnentag, O., & Toomey, M. (2013). Climate change, phenology, and phenological control of vegetation feedbacks to the climate system. *Agricultural and Forest Meteorology*, *169*, 156–173. https://doi.org/10.1016/j.agrformet.2012.09.012

Running, S. W., & Hunt, E. R. Jr. (1993). *Generalization of a forest ecosystem process model for other biomes, BIOME-BCG, and an application for global-scale models* (pp. 141–158). San Diego, CA: Academic Press. Retrieved from http://secure.ntsg.umt.edu/publications/1993/RH93/

Running, S. W., Nemani, R. R., & Hungerford, R. D. (1987). Extrapolation of synoptic meteorological data in mountainous terrain and its use for simulating forest evapotranspiration and photosynthesis. *Canadian Journal of Forest Research*, *17*(6), 472–483. https://doi.org/10.1139/x87-081

Scaife, C. I., & Band, L. E. (2017). Nonstationarity in threshold response of stormflow in southern Appalachian headwater catchments. *Water Resources Research*, *53*, 6579–6596. https://doi.org/10.1002/2017WR020376

Tague, C. L. (2009). Assessing climate change impacts on alpine stream-flow and vegetation water use: Mining the linkages with subsurface hydrologic processes. *Hydrological Processes*, *23*(12), 1815–1819. https://doi.org/10.1002/hyp.7288

Tague, C. L., & Band, L. E. (2004). RHESSys: Regional Hydro-Ecologic Simulation System—An object-oriented approach to spatially distributed modeling of carbon, water, and nutrient cycling. *Earth Interactions*, *8*(19), 1–42. https://doi.org/10.1175/1087-3562(2004)8%3C1:RRHSSO%3E2.0.CO;2

Tague, C. L., Grant, G., Farrell, M., Choate, J., & Jefferson, A. (2008). Deep groundwater mediates streamflow response to climate warming in the Oregon Cascades. *Climatic Change*, *86*(1–2), 189–210. https://doi.org/10.1007/s10584-007-9294-8

Tague, C. L., & Grant, G. E. (2009). Groundwater dynamics mediate low-flow response to global warming in snow-dominated alpine regions. *Water Resources Research*, *45*, W07421. https://doi.org/10.1029/2008WR007179

Tague, C. L., McMichael, C., Hope, A., Choate, J., & Clark, R. (2004). Application of the RHESSys model to a California semiarid shrubland watershed. *Journal of the American Water Resources Association*, *40*(3), 575–589. https://doi.org/10.1111/j.1752-1688.2004.tb04444.x

The MathWorks, I. (2000). MATLAB 8.1 and Statistics Toolbox 8.1. Natick, MA.

Thompson, S. E., Harman, C. J., Konings, A. G., Sivapalan, M., Neal, A., & Troch, P. A. (2011). Comparative hydrology across AmeriFlux sites: The variable roles of climate, vegetation, and groundwater. *Water Resources Research*, *47*, W00J07. https://doi.org/10.1029/2010WR009797

Troch, P. A., Martinez, G. F., Pauwels, V. R. N., Durcik, M., Sivapalan, M., Harman, C., et al. (2009). Climate and vegetation water use efficiency at catchment scales. *Hydrological Processes*, *23*(16), 2409–2414. https://doi.org/10.1002/hyp.7358

Urbanski, S. P., Barford, C., Wofsy, S., Kucharik, C. J., Pyle, E., Budney, J., et al. (2007). Factors controlling CO_2 exchange on timescales from hourly to decadal at Harvard Forest. *Journal of Geophysical Research*, *112*, G02020. https://doi.org/10.1029/2006JG000293

Vicente-Serrano, S. M., Camarero, J. J., Zabalza, J., Sangüesa-Barreda, G., López-Moreno, J. I., & Tague, C. L. (2015). Evapotranspiration deficit controls net primary production and growth of silver fir: Implications for Circum-Mediterranean forests under forecasted warmer and drier conditions. *Agricultural and Forest Meteorology*, *206*, 45–54. https://doi.org/10.1016/j.agrformet.2015.02.017

Walther, G.-R., Post, E., Convey, P., Menzel, A., Parmesan, C., Beebee, T. J. C., et al. (2002). Ecological responses to recent climate change. *Nature*, *416*(6879), 389–395. https://doi.org/10.1038/416389a

Weider, K., & Boutt, D. F. (2010). Heterogeneous water table response to climate revealed by 60 years of ground water data. *Geophysical Research Letters*, *37*, L24405. https://doi.org/10.1029/2010GL045561

White, M. A., & Nemani, R. R. (2003). Canopy duration has little influence on annual carbon storage in the deciduous broad leaf forest. *Global Change Biology*, *9*(7), 967–972. https://doi.org/10.1046/j.1365-2486.2003.00585.x

White, M. A., Running, S. W., & Thornton, P. E. (1999). The impact of growing-season length variability on carbon assimilation and evapotranspiration over 88 years in the eastern US deciduous forest. *International Journal of Biometeorology*, *42*(3), 139–145. https://doi.org/10.1007/s004840050097

White, M. A., Thornton, P. E., Running, S. W., & Nemani, R. R. (2000). Parameterization and sensitivity analysis of the BIOME–BGC terrestrial ecosystem model: Net primary production controls. *Earth Interactions*, *4*(3), 1–85. https://doi.org/10.1175/1087-3562(2000)004<0003:PASAOT>2.0.CO;2

Wigmosta, M. S., Vail, L. W., & Lettenmaier, D. P. (1994). A distributed hydrology-vegetation model for complex terrain. *Water Resources Research*, *30*(6), 1665–1679. https://doi.org/10.1029/94WR00436

Wilson, K. B., & Baldocchi, D. D. (2000). Seasonal and interannual variability of energy fluxes over a broadleaved temperate deciduous forest in North America. *Agricultural and Forest Meteorology*, *100*, 1–18. https://doi.org/10.1016/S0168-1923(99)00088-X

Yu, Z., Lu, C., Cao, P., Tian, H., Hessl, A., & Pederson, N. (2018). Earlier leaf-flushing suppressed ecosystem productivity by draining soil water in the Mongolian Plateau. *Agricultural and Forest Meteorology*, *250–251*, 1–8. https://doi.org/10.1016/j.agrformet.2017.11.035

Zhang, X., Friedl, M. A., Schaaf, C. L., Strahler, A. H., Hodges, J. C. F., Gao, F., et al. (2003). Monitoring vegetation phenology using MODIS. *Remote Sensing of Environment*, *84*(3), 471–475. https://doi.org/10.1016/S0034-4257(02)00135-9

Zierl, B., Bugmann, H., & Tague, C. L. (2007). Water and carbon fluxes of European ecosystems: An evaluation of the ecohydrological model RHESSys. *Hydrological Processes*, *21*(24), 3328–3339. https://doi.org/10.1002/hyp.6540